

AD-A152 227

PREDICTING FULLY PLASTIC MODE II CRACK GROWTH FROM AN
ASYMMETRIC DEFECT(U) MASSACHUSETTS INST OF TECH
CAMBRIDGE DEPT OF MECHANICAL ENGIN..
F A MCCLINTOCK ET AL. 28 FEB 85

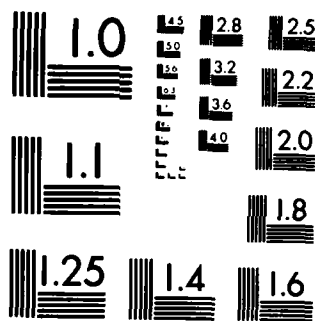
1/1

UNCLASSIFIED

F/G 20/11

NL

								END					
								FILED					
								DTB					



MICROCOPY RESOLUTION TEST CHART
NATIONAL BUREAU OF STANDARDS-1963-A

②

Technical Report N00014-82-K-0025 P00002 TR01

PREDICTING FULLY PLASTIC MODE II CRACK GROWTH FROM AN ASYMMETRIC DEFECT

Frank A. McClintock

Room 1-304, (617) 253-2219
Department of Mechanical Engineering
Massachusetts Institute of Technology
Cambridge, MA 02139

Alexander H. Slocum, now at

Bldg. 233, Room B108, (301) 921-3381
National Bureau of Standards
U.S. Department of Commerce
Gaithersburg, MD 20899

Unlimited Distribution

28 February 1985

Technical Report

Prepared for

OFFICE OF NAVAL RESEARCH
Solids Mechanics Program, Mechanics Division
Scientific Officer: Dr. Yapa Rajapakse
Code 432S (202) 696-4306
800 N. Quincy Street
Arlington, VA 22217

DTIC
ELECTE
APR 08 1985
S D
E

AD-A152 227

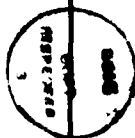
DTIC FILE COPY

85 03 18 068

REPORT DOCUMENTATION PAGE		READ INSTRUCTIONS BEFORE COMPLETING FORM
1. REPORT NUMBER N00014-82-K-0025 P00002 TR01	2. GOVT ACCESSION NO.	3. RECIPIENT'S CATALOG NUMBER
4. TITLE (and Subtitle) PREDICTING FULLY PLASTIC MODE II CRACK GROWTH FROM AN ASYMMETRIC DEFECT	5. TYPE OF REPORT & PERIOD COVERED Technical Report 28 February 1985	
	6. PERFORMING ORG. REPORT NUMBER	
7. AUTHOR(s) Frank A. McClintock Alexander H. Slocum (now at Natl. Bur. Stds. -- Bldg 233 Room B108 Gaithersburg, MD 20899	8. CONTRACT OR GRANT NUMBER(s) N00014-82-K-0025 P00002	
9. PERFORMING ORGANIZATION NAME AND ADDRESS Department of Mechanical Engineering Massachusetts Institute of Technology Cambridge, MA 02139	10. PROGRAM ELEMENT, PROJECT, TASK AREA & WORK UNIT NUMBERS Work unit NR 064-679	
11. CONTROLLING OFFICE NAME AND ADDRESS Office of Naval Research Solid Mechanics Program, Mech. Div. Code 432S 800 N. Quincy Street, Arlington, VA 22217	12. REPORT DATE 28 February 1985	
	13. NUMBER OF PAGES 38	
14. MONITORING AGENCY NAME & ADDRESS (if different from Controlling Office)	15. SECURITY CLASS. (of this report) Unclassified	
	15a. DECLASSIFICATION/DOWNGRADING SCHEDULE	
16. DISTRIBUTION STATEMENT (of this Report) Distribution Unlimited		
17. DISTRIBUTION STATEMENT (of the abstract entered in Block 20, if different from Report)		
18. SUPPLEMENTARY NOTES Accepted by International Journal of Fracture		
19. KEY WORDS (Continue on reverse side if necessary and identify by block number) Ductile fracture, fully plastic, mixed mode, crack initiation, crack growth, Mode I, Mode II, asymmetry, crack ductility, weld defects, shear band, theory, experiments, oblique, shear lip		
20. ABSTRACT (Continue on reverse side if necessary and identify by block number) Asymmetrically cracked specimens fail with considerably less ductility than symmetrically cracked ones, due to the crack progressing along a shear band into pre-damaged material. A formulation for the accumulation of damage ahead of an asymmetric crack is presented, based on strain increments following a power law relation. These results are integrated both numerically and approximately. The crack growth per unit displacement increases approximately as the		

logarithm of the total crack advance per inclusion spacing λ and varies inversely as the critical fracture strain ϵ_c . This provides a basis for predicting large-scale, fully plastic fracture from asymmetric weld defects, using small-scale laboratory specimens.

Originator - supplied key words included: front



Accession For	
NTIS GRA&I	<input checked="" type="checkbox"/>
DTIC TAB	<input type="checkbox"/>
Unannounced	<input type="checkbox"/>
Justification	
By	
Distribution/	
Availability Codes	
Dist	Avail and/or Special
A-1	

(Accepted by International Journal of Fracture)

Predicting Fully Plastic Mode II Crack Growth from an Asymmetric Defect

by

Frank A. McClintock¹ and Alexander H. Slocum²

ABSTRACT

Asymmetrically cracked specimens fail with considerably less ductility than symmetrically cracked ones, due to the crack progressing along a shear band into pre-damaged material. A formulation for the accumulation of damage ahead of an asymmetric crack is presented, based on strain increments following a power law relation. These results are integrated both numerically and approximately.

The crack growth per unit displacement increases approximately as the logarithm of the total crack advance per inclusion spacing ϕ , and varies inversely as the critical fracture strain γ_c . This provides a basis for predicting large-scale, fully plastic fracture from asymmetric weld defects, using small-scale laboratory specimens.

¹Professor, Department of Mechanical Engineering, Room 1-304, Massachusetts Institute of Technology, Cambridge MA 02139, U.S.A.

²Graduate Student, Department of Mechanical Engineering, Room 3-382, Massachusetts Institute of Technology, Cambridge MA 02139, U.S.A., currently with the National Bureau of Standards, U.S. Department of Commerce, Gaithersburg, Maryland 20899

1. Introduction

Most fracture tests use symmetric specimens. The crack tends to advance into the relatively undamaged region between two plastic shear zones. In the fully plastic case, which is the desirable one in a structure, these zones narrow into bands that traverse the section. In practice, welds or other asymmetries may eliminate one of the shear bands (Fig. 1). In that case, the crack advances along a single shear band into previously damaged material. Thus one might expect that the ductility would be less. Preliminary experiments have shown that this is indeed the case. Further evidence for a lowered ductility in asymmetric cracking is the tendency to form a shear lip at the end of an ordinary cup-and-cone fracture in a tensile test.

A plastic fracture mechanics analysis would be helpful in predicting such fractures in service from laboratory tests on small specimens. The observations of Beachem and Meyn [1] and Fellows et al. [2], that fracture occurs by a mixture of hole growth and sliding off, suggest using the fracture criterion of McClintock, et al. [3] for fracture by hole growth in a shear band.

The required strain might first be sought from a non-hardening plasticity solution. Non-hardening plasticity, however, indicates a single shear band with a constant displacement discontinuity and hence infinite strain across it. Any fracture criterion would therefore be satisfied simultaneously all along the shear band; total fracture would occur immediately upon any crack growth.

Strain-hardening causes the band to spread out, leaving a finite

strain except at the very tip. Shih [4] gave a non-linear elastic solution for a stationary crack under combined shear and tension. This solution will be used to estimate the displacement required to advance the crack (which is that to develop the critical strain or damage at a point one inclusion spacing ahead of the current crack tip).

For growth, the same fracture criterion can be used. However, no solution exists for determining the distribution of strain increments as the crack advances into pre-strained material. An approximation will therefore be developed from Shih's non-linear elastic solution. The crack will be assumed to follow the center of a 45° shear band.

This simplified, one-dimensional model should provide insight for estimating fractures in service, and developing a more realistic two-dimensional analysis for a crack growing in rigid-plastic, strain-hardening material.

2. Analysis

In treating Mode II shear, Shih [4] defined the stress-strain relation for a hardening material in terms of the yield strain σ_0/E , the strain hardening exponent $1/m$, and a constant α :

$$\sigma = \sigma_0 \left(\frac{E}{\sigma_0 \alpha} \right)^{1/m} \epsilon^{1/m} . \quad (1)$$

For general mixed-mode, non-linear elastic behavior, Shih found the strain ahead of the crack in terms of a Mode I "mixity parameter" M^D , the far-field linear elastic stress intensity factor for mixed Mode I and Mode II K_M , the distance r ahead of the crack tip, and a normalized strain

Printer's
note:
K sub-
script M

Super-
script of
1

which depends on the orientation of a point relative to the shear band,
 $\tilde{\epsilon}_{ij}^P(\theta, M^P)$:

$$\epsilon_{ij}^P = \frac{\alpha \sigma_0}{E} (K_{MP})^m r^{-m/(m+1)} \tilde{\epsilon}_{ij}^P(\theta, m, M^P) . \quad (2)$$

Our problem is fully plastic, so the stress intensity factor is restated in terms of the J-integral, and a function $I_m(M^P)$ [4]:

$$J = \frac{\alpha \sigma_0^2}{E} I_m(M^P) (K_{MP})^{m+1} . \quad (3)$$

The relation between the J integral and the fully plastic strain distribution depends only on the fully plastic part of the stress-strain relation; therefore, it is more convenient to use the Swift [5] equation, in terms of the flow stress at unit strain rather than the yield strength:

$$\sigma = \bar{\sigma}_1 \epsilon^n . \quad (4)$$

Equating (1) and (4) with $n = 1/m$ gives

$$\bar{\sigma}_1 = \sigma_0 \left(\frac{E}{\sigma_0 \alpha} \right)^n . \quad (5)$$

Substitution of (5) and (3) into (2) eliminates the initial yield variables σ_0 and α in terms of the flow stress at unit strain $\bar{\sigma}_1$, which is more appropriate for the fully plastic singularity:

$$\epsilon_{ij}^P(r, \theta) = \left(\frac{J}{\bar{\sigma}_1 I_{1/n}(M^P) r} \right)^{\frac{1}{n+1}} \tilde{\epsilon}(\theta, 1/n, M^P) . \quad (6)$$

Equation 6 is a modified form of that given by Hutchinson [6] and Rice and Rosengren [7] for the non-linear elastic, Mode I strain distribution ahead

of a crack tip.

The path independent integral J is evaluated from its definition in terms of its coordinates x_1, x_2 parallel and normal to the crack, the work per unit volume U , tractions T_j , and displacements u_i along the boundary s :

$$J \equiv \int U dx_2 - T_j \frac{\partial u_j}{\partial x_1} ds. \quad (7)$$

For rigid-nonhardening plasticity, the work per unit volume U is zero except where the shear band cuts the surface. There it is given in terms of the shear strength k and strain γ by

$$U = k\gamma. \quad (8)$$

From Fig. 1b, for a relative displacement u across a shear band of thickness τ ,

$$\gamma = \frac{u}{\tau}. \quad (9)$$

The x_2 distance is

$$\delta x_2 = \tau, \quad (10)$$

so the first term of the J -integral (7) becomes ku . The displacement u is constant along the grips (or outer boundaries, the only place the tractions T are non-zero), so

$$\frac{\partial u_j}{\partial x_1} = 0 \text{ unless } T = 0. \quad (11)$$

Thus the second term of (7) vanishes everywhere, leaving

$$J = ku \quad . \quad (12)$$

Substituting (12) into (6) gives

$$\epsilon_{ij}^p(r, \theta) = \left(\frac{ku}{\bar{\sigma}_1 I_{1/n}(M^p) r} \right)^{\frac{1}{n+1}} \tilde{\epsilon}_{ij}(\theta, 1/n, M^p) \quad . \quad (13)$$

Initiation of crack growth. Crack growth is assumed to begin when a critical shear strain γ_c is reached at a distance ρ , say one inclusion spacing, ahead of the crack tip.

McClintock, Kaplan, and Berg [8] expressed the condition for shear fracture in terms of a damage η , depending on the shear strain γ , a hole growth factor F_T , the ratio of mean normal to maximum shear stress σ/τ , and the strain hardening exponent n :

$$\eta = 1 = \frac{1}{2nF_T} \ln \sqrt{1 + \gamma^2} + \frac{\gamma}{2(1-n)} \sinh \frac{(1-n)\sigma}{\tau} \quad . \quad (14)$$

For non-hardening plasticity far from the crack tip, the loading of Fig. 1 gives $\sigma/\tau = 1$. Closer to the tip the normal stress σ/τ will be relaxed by local normal strains associated with any normal stress and the dominant shear mode. Thus the critical shear strain at a point on the shear band to cause the crack to grow, (14), reduces to

$$2\epsilon_{r\theta} = \gamma_c = \sqrt{F_T^2 - 1} \quad . \quad (15)$$

The displacement to initiate crack growth, u_1 , is found by solving

(13) in terms of $\epsilon_{ij} = \gamma/2$. At the same time, take $\theta = 0$ along the shear band and the Mode I mixity M^P to be zero since $\sigma/\tau = 0$:

$$u_i = \frac{\bar{\sigma}_1 I_{1/n}}{k} r \left(\frac{\gamma(r)}{2\tilde{\epsilon}_{ij}} \right)^{n+1}_{r=\rho, \gamma=\gamma_c} \quad (16)$$

The strain along the shear band ahead of the crack tip is then

$$\frac{\gamma(r)}{\gamma_c} = \left(\frac{\rho}{r} \right)^{\frac{1}{n+1}} \quad (17)$$

After the crack advance, the strain ρ ahead of the new crack tip is less than γ_c (Fig. 2). In the rigid-plastic material, no strain occurs from the stress redistribution due to crack growth, so a further displacement is required for further crack growth. Unfortunately, no solution exists yet for the strain ahead of a crack that is growing into hardening material. Equation 16 is based on deformation plasticity which would not account for the changing stress and accumulated strain-hardening around the crack tip.

An approximation for the strain can be obtained by differentiating (16) with respect to the strain increment, in terms of the radius r to a point and the current strain there:

$$\frac{du}{d\gamma(r)} = \frac{(n+1)\bar{\sigma}_1 I_{1/n}}{2k\tilde{\epsilon}_{ij}} r \left(\frac{\gamma(r)}{2\tilde{\epsilon}_{ij}} \right)^n \quad (18a)$$

Normalizing the displacement with that for initiation from (16) and normalizing the strains with γ_c and the coordinates with ρ gives

$$\frac{d(u/u_1)}{d(\gamma(r)/\gamma_c)} = (n+1)(r/\rho)(\gamma(r)/\gamma_c)^n . \quad (18b)$$

Denote normalized variables by (*):

$$\frac{du^*}{d\gamma^*(r^*)} = (n+1)r^*(\gamma^*(r^*))^n . \quad (18c)$$

For simplicity, delete (*), so $u/u_1 \rightarrow u$, etc.:

$$\frac{du}{d\gamma(r)} = (n+1)(\gamma(r))^n r . \quad (18d)$$

For numerical integration with a finite Δc , the new strain field ahead of a growing crack can be found by integrating the reciprocal of (18):

$$\gamma_{new}^{n+1}(r) = \gamma_{old}^{n+1}(r) + \Delta u/r , \quad (19)$$

The strain γ_{new} at $r = 1$ ahead of the new crack tip must reach the normalized value of unity, for the crack to advance farther. From (19), the required displacement increment is

$$\Delta u_c = 1 - \gamma_{old}^{n+1}(1) . \quad (20)$$

The strain at any other point on the shear band is

$$\gamma_{new}^{n+1}(r) = \gamma_{old}^{n+1}(r) + [1 - \gamma_{old}^{n+1}(1)]/r_{ave} . \quad (21)$$

Note that in (20) and (21), $\gamma^{n+1}(r)$ could be replaced by any other damage function η whose radial distribution also satisfies (21), without changing the normalized growth rate. The strain hardening exponent n would

not appear. Therefore, when the equations are normalized by dividing by u_i , which is proportional to γ_c^{n+1} , the displacement required for a given crack growth $c - c_i$ is independent of the strain hardening exponent n .

Before numerically integrating these equations, consider the possibility of a quasi-steady-state solution.

3. A Quasi-Steady-State Solution

In general the strain at r ahead of a crack that has grown from c_i through ξ to c is

$$\gamma(r, c) = \int_{\xi=c_i}^{\xi=c} \frac{d\gamma}{du} \frac{du}{d\xi} d\xi. \quad (22)$$

If a quasi-steady state solution exists ($du/d\xi \approx du/dc$), then (18d) with $r \rightarrow r + (c - \xi)$ and (22) give

$$\gamma(r, c) = \frac{du}{dc} \int_{\xi=c_i}^{\xi=c} \frac{d\xi}{(n+1)(r+c-\xi)(\gamma(r+c-\xi))^n}. \quad (23)$$

Assuming a solution of the form

$$\gamma(r+c-\xi) = (r+c-\xi)^{-\lambda} \quad (24)$$

with $\lambda > 0$ gives, for (23),

$$\frac{1}{r^\lambda} = \frac{du}{dc} \frac{1}{(n+1)} \int_{c_i}^c (c+r-\xi)^{\lambda n - 1} d\xi. \quad (25)$$

Integrating (25) gives

$$\frac{1}{r^\lambda} = \frac{du}{dc} \frac{1}{(n+1)\lambda n} [(c+r-c_i)^{\lambda n} - r^{\lambda n}] . \quad (26)$$

At best, (26) is satisfied for a variety of r only if $\lambda \ll 1$. Then using

$$x^\lambda = e^{\lambda \ln x} = 1 + \lambda \ln x \quad (27)$$

in (26) gives, for $\lambda \ln r \ll 1$

$$1 = \frac{du}{dc} \frac{1}{(n+1)} [\ln(c-c_i+r) - \ln r] . \quad (28)$$

Near the crack tip (for $r \sim 1$ ($=\rho$, when de-normalized)) and after large growth ($c-c_i \gg 1$), solving for du/dc gives

$$\frac{du}{dc} = \frac{n+1}{\ln(c-c_i+1)} . \quad (29)$$

As it stands, (29) gives an infinite displacement rate at $c = c_i$. Since the initiation strain was neglected in (22), (29) should be modified to fit the initial displacement rate per unit crack growth from the more exact solution. From Fig. 2, the drop in strain from ρ to $\rho + dc$ in front of the crack must be made up by the displacement required for further growth:

$$\left| \frac{d\gamma}{dr} \right| dc = \frac{d\gamma}{du} du . \quad (30)$$

The initial strain gradient is found from (17) in normalized form:

$$\left| \frac{d\gamma}{dr} \right| = \frac{1}{n+1} \left(\frac{1}{r} \right)^{1/(n+1) + 1} = \frac{1}{n+1} \text{ at } r = 1 . \quad (31)$$

The displacement required per unit strain at a normalized $r = 1$ is found from (18d) at a normalized $\gamma = 1$:

$$\frac{du}{d\gamma} = n + 1 . \quad (32)$$

Combining (30) - (32) gives a result that can be matched to (29) at $c = c_1$:

$$\left[\frac{du}{dc} = \frac{|d\gamma/dr|}{d\gamma/du} = 1 \right]_{c=c_1} \quad \text{if} \quad \frac{du}{dc} = \frac{n+1}{\ln(c - c_1 + \exp(n+1))} . \quad (33)$$

The integral of (33) to find the quasi-static displacement since initiation is carried out with the intermediate variable

$$y \equiv \ln(\xi - c_1 + \exp(n+1)) : \quad (34)$$

$$\begin{aligned} u_{qs} - 1 &= \int_{c_1}^c \frac{(n+1)d\xi}{\ln(\xi - c_1 + \exp(n+1))} \\ &= (n+1) \left[\ln y + y + \frac{y^2}{2 \cdot 2!} + \frac{y^3}{3 \cdot 3!} + \dots \right]_{n+1}^{y(c)} . \end{aligned} \quad (35)$$

To determine convergence, consider the ratio of adjacent terms:

$$t_j = t_{j-1} \frac{y(j-1)}{j} . \quad (36)$$

Thus the sum of the remaining terms is bounded by

$$s_r = \sum_j t_j = \left[\frac{y(j-1)}{j} + \frac{y^2(j-1)}{j(j+1)^2} + \frac{y^3(j-1)}{j(j+1)(j+2)^2} + \dots \right] t_{j-1} ;$$

$$s_r < t_{j-1} \left[\frac{y}{j} + \left(\frac{y}{j}\right)^2 + \left(\frac{y}{j}\right)^3 + \dots \right],$$

$$s_r < t_{j-1} / (1 - y/j) \text{ for } j > y. \quad (37)$$

A sufficient number of terms has been evaluated when

$$\frac{s_r}{u_{qs}} \equiv \epsilon_t < \epsilon_{tol}. \quad (38)$$

4. Numerical Integration

To establish an array of strain sites on the shear band ahead of the crack tip, choose the first site such that, before growth by Δc , the site is $\rho + \Delta c/2$ ahead of the current crack tip, and after growth, only $\rho - \Delta c/2$ ahead. Define Δc as a binary fraction of ρ in terms of an integer N_{dc} :

$$\Delta c = \rho / 2^{N_{dc}}. \quad (39)$$

Set the next damage site a distance Δc from the first site. Since the damage decreases rapidly with distance ahead of the crack tip, no accuracy is lost, and large computational time savings are achieved, by initially doubling the intervals between sites (see Fig. 3). Thus use spacings of Δc , $2\Delta c$, $4\Delta c$, The initial number of damage sites, ix_{dmx} , is expressed in terms of the initial ligament length L_i :

$$ix_{dmx} = 2 + \text{INT} \left(\frac{\log \left(\frac{L_i - \rho - \Delta c/2}{\Delta c} \right)}{\log(2)} \right). \quad (40)$$

The maximum number of sites is bounded by twice the value given by (40).

In the program, the damage at each site is calculated from (19) as if the crack were at its average position, ρ before the first damage site.

As the crack grows, the old second site becomes the new first site. The old third site is more than Δc away from the new first site, so a new site is introduced midway between the two. Further from the crack tip, whenever the ratio of the distances between neighboring pairs of sites exceeds 2, a new site is introduced.

Hyperbolic interpolation is used to find the damage and strain at any new sites. In terms of the coordinates x_1 , x_2 at the old sites either side of the new site, the value at the new site is:

$$y = y_1 (x_1 - c)/(x - c)^B, \quad (41)$$

where

$$B = \frac{\log(y_1/y_2)}{\log[(x_2 - c)/(x_1 - c)]} \quad (42)$$

The above analysis was carried out with a well-annotated FORTRAN-IV computer program, in structured form with BLOCK IF statements. It is available at cost, with a User's Manual and sample problem, on unformatted ASCII tape [9].

5. Results and Discussion

a) Strain distribution. As shown in Fig. 4, the strain distribution continually flattens out in front of the crack at a decreasing rate that does not reach a steady state. This leads to a continually increasing crack growth rate per unit displacement.

b) Crack growth rate. The absence of any effect of strain hardening on crack growth rate was verified by the numerical integration, which was programmed in the original un-normalized form. The results for various step sizes converge rapidly, as shown in Fig. 5, with a 4% error associated with crack growth increments of $\Delta c/\rho = 1/8$.

The incorrect dependence of the quasi-steady-state approximation on the strain hardening exponent n leads to an overestimate by about a factor of $(1.1 + n)$.

c) Size effects. As shown by (29), the crack growth per unit displacement increases logarithmically with the total crack growth. Thus no steady state is reached, as shown in Fig. 6, which extends to a crack growth of $(c - c_1)/\rho = 10^4$, (corresponding to a fracture process zone size $\rho = 0.01$ mm and a total cross-section of 100 mm). The availability of such a curve allows estimating the displacement to cause fracture of large specimens from tests on small samples. For example, the ratio of the crack growth rate for a prototype part (e.g. Fig. 6) to that for a laboratory specimen (e.g. Fig. 5) is approximately

$$\left(\frac{dc}{du}\right)_{\text{prot}} / \left(\frac{dc}{du}\right)_{\text{lab}} = \frac{\ln((c - c_1)/\rho)_{\text{prot}}}{\ln((c - c_1)/\rho)_{\text{lab}}} = \frac{\ln 10000}{\ln 200} \approx 1.7 \quad (43)$$

d) Initiation displacement from material properties. For the initiation displacement of (16), the normalized shear strain $\tilde{\epsilon}_{ij}$ and the coefficient $I_{1/n}$ are given as functions of the strain hardening exponent in Table 1 from Shih [4]. Since the strain hardening exponent is small compared to unity, these values, when substituted into (16), indicate that the displacement for initiation is of the order of the inclusion spacing ρ times the critical strain to fracture γ_c . Equation (33) then indicates that, in the un-normalized form, the crack growth per unit displacement is of the order

$$\frac{dc}{du} = O\left(\frac{1}{\gamma_c} \ln \frac{c - c_i}{\rho}\right). \quad (44)$$

e) Preliminary experiments. The results of preliminary experiments are summarized in Table 2. The critical fracture strain for these alloys (except for the 6061-T6) can be estimated from the different lengths of the two displacement crack surfaces by averaging them to get the crack growth to fracture, $(s_2 + s_1)/2 = c_f - c_i$, and taking their differences to get the displacement across the shear band at fracture, $s_2 - s_1 = u_f$. Fractographic estimates of ρ then allow calculating u_i from the function F of Figs. 5 and 6:

$$u_f/u_i = F\left\{(c_f - c_i)/\rho\right\}; \quad u_i = u_f/(u_f/u_i). \quad (45)$$

Solving (16) for γ_c at $r = \rho$ allows finding the critical fracture strain:

$$\gamma_c = 2 \tilde{\epsilon}_{ij} \left(\frac{u_i}{\rho} \frac{1}{(\bar{\sigma}_1/k) I_{1/n}} \right)^{1/(n+1)}. \quad (46)$$

(Note that in these tests the actual initiation displacement would not be that calculated above, because the shear band was at 45° to the initial

crack.) The results, given in Table 2, are plausible except for the high strength 6061-T6 alloy, discussed below in Paragraph f. It should be noted further that these calculations were made under the assumption that the crack grew along the center of the shear band at 45° to the tensile axis. There was a tendency for the angle to be somewhat greater than 45° , giving a higher triaxiality σ/k . This would reduce the critical strain to fracture. The fracture strain may be further reduced by the localization of flow. In simple shear, as here in Mode II and also in torsion, such localization is accelerated by the strain softening that occurs when the strain increment reverses sign on those slip planes that rotate past the 45° direction (planes at 45° to the axes of macroscopic shear do not slip; those at less than 45° slip one way, while those at more than 45° slip the other). Furthermore, the preferred orientation that develops in simple shear promotes single slip and thus also reduces strain hardening.

f) Elastic and blunting effects. A rough estimate of the effect of elasticity on the above comparison of the rigid-plastic analysis with experiments will be made on the basis of Mode III which, like the mixed Modes I and II but in contrast to pure Mode I, shows an extended plastic zone ahead of the crack.

Before crack growth, the predominant elastic-plastic effect occurs as the plastic zone grows across the specimen through the distance L . The resulting plastic strain at the structural distance ρ is, from (2b) of [3],

$$\gamma_{ep1} = \gamma_y(L/\rho - 1) \quad . \quad (47)$$

Approximating the shear yield strain γ_y with $Bhn/3E$, taking L to be the average surface length $(s_1+s_2)/2$, and substituting numerical values from Table 2 into (47) gives strains of the order of half the critical (fracture) strains γ_c . Therefore, the elastic-plastic strain is important, and decreases the fully plastic displacements required for initiation, u_1 , below those found in Table 2. Blunting effects, on the other hand, which are neglected in the rigid-plastic analysis, tend to increase u_1 .

During crack growth, with a contained plastic zone of extent R the elastic-plastic strain is, from (10) of [3],

$$\left(\frac{\partial \gamma_{ep}}{\partial c}\right)_{r=\rho} = \frac{\gamma_y}{\rho} \left(1 + \frac{R}{c} + \ln \frac{R}{\rho}\right), \quad (48)$$

which is to be compared to that from the rigid-plastic analysis,

$$\frac{\partial \gamma_p}{\partial c} = \frac{d\gamma_p/du}{dc/du}, \quad (49)$$

where the numerator is found from (18d) and the denominator from (33), (which are normalized with γ_c , ρ , and u_1).

At the start of growth, with $R \approx c = 0$ ($L = 2.5$ mm), (48) gives an elastic-plastic strain per unit crack growth of 0.7 to 2.2 mm^{-1} , while (49) gives a corresponding fully plastic strain of 45 to 26 mm^{-1} . Thus the rigid-plastic approximation is initially very good.

Later when the crack has grown almost completely through ($c-c_1 = L = 2.5$ mm), the fully plastic strain from (49) decreases by about a factor of 5 to 10 to 6 mm^{-1} . This should be compared with the elastic-plastic strain

per unit growth. Equation (48) no longer applies when the plastic zone has traversed the specimen, but it seems likely that the strain per unit growth continues to increase as the slip band intensifies. Thus the rigid-plastic approximation will ultimately become poor as the crack grows, although a very large specimen would be required for instability under contained yielding. (More formal estimates might be made from the speculations of Rice et al. [10, p. 204]).

The instability that precluded getting data for the 6061-T6 may have been due to the compliance of the testing machine, rather than to elastic-plastic strains in the ligament. Consider the following argument. Let K denote the combined machine and grip stiffness; it is the drop in applied load per unit specimen extension. The load drop in the net section due to a crack growth dc is roughly given in terms of the tensile strength of the material TS and the breadth of the specimen B by $TS B dc$. Then for stability

$$K > - \frac{dP}{du} = \frac{B TS}{du/dc} \quad (50)$$

Although comparison of the right-hand sides of (50) for the different alloys explains the stability with 6061-O, it fails to distinguish between the stability with the cold rolled steel and the instability with the 6061-T6 aluminum alloy. While the effect of extra compliance in the shoulders of the aluminum on K is a possible explanation, further work is needed for certainty.

Printers
note: "O"
in 6061-O

6. Conclusions

1. An estimate of fully plastic Mode II crack growth along 45° slip bands, as might be encountered from cracks near a weld, was developed from Shih's analysis for nonlinear elastic behavior. The results appear plausible when compared to preliminary experiments on several alloys and heat treatments. Elastic effects appear to become important in harder alloys such as 6061-T6, with an elastic strain at the tensile strength of $\epsilon_s/E = 0.006$.

2. From the rigid-plastic theory, the predicted displacement to crack initiation is of the order of the inclusion spacing ρ times the critical strain to fracture γ_c .

3. The crack growth per unit displacement is of the order of the logarithm of the total crack advance per unit inclusion spacing ρ , divided by the critical fracture strain γ_c , equation (44).

4. The relation between displacement for a given crack advance and critical fracture strain is relatively independent of the strain hardening exponent n and inclusion spacing ρ , so that the critical fracture strain can be found from crack growth data, equation (44).

5. The results indicate how to extrapolate tests on laboratory specimens to prototype parts. For instance the crack growth per unit displacement after a 100 mm crack growth appears to be about twice that after a 2 mm growth, equation (29).

6. There are needs for more detailed and comprehensive experiments, a study of the directional effects, a solution to the singular strain distribution ahead of a crack growing in rigid-plastic, strain-hardening material, and finally an elastic-plastic analysis.

7. Acknowledgements. We wish to thank George Dvorak for enthusiasm and skill in designing the experimental apparatus and carrying out preliminary tests, Bill Carter for help in comparing analysis with data, George Kardomateas for reviewing the manuscript, and Martha Adams and Saechin Kim for typing the manuscript and revisions to final form. We acknowledge with thanks the support of the Office of Naval Research, Structural Mechanics Program Code 432, Arlington, Virginia, Contract W0014-82K-0025. We are especially grateful to the project monitor, Dr. Y. Rajapakse, for his interest in this work. The numerical analysis was carried out by AHS as a B.S. thesis, Department of Mechanical Engineering, M.I.T.

8. References.

- [1] Beachem, C.D. and Meyn, D.A. (1968), "Fracture by Microscopic Plastic Deformation Processes," Electron Fractography, ASTM STP 436, Am. Soc. Test Mat., Philadelphia, pp. 58-88.
- [2] Fellows, J.A., ed. (1974), "Interpretation of Transmission-Electron-Microscope Fractographs," Metals Handbook, 8th ed.: Fractography and Atlas of Fractographs, Amer. Soc. for Metals, Metals Park, Ohio, pp. 79-92.
- [3] McClintock, F.A. (1958), "Ductile Fracture Instability in Shear," J. Appl. Mech., v. 25, 581-588.
- [4] Shih, C.F. (1974), "Small Scale Yielding Analysis of Mixed Mode Plane-Strain Crack Problems," Fracture Analysis, ASTM STP 560, Am. Soc. Test Mat., Philadelphia, pp. 187-210.
- [5] Swift, H.W. (1952), "Plastic Instability Under Plane Stress," J. Mech. Phys. Solids, v. 1, 1-18.
- [6] Hutchinson, J.W. (1968), "Singular Behavior at the End of a Tensile Crack in a Hardening Material", J. Mech. Phys. Solids, v. 16, 13-31.
- [7] Rice, J.R., and Rosengren, G.F. (1968), "Plane Strain Deformation Near a Crack Tip in a Power-Law Hardening Material," J. Mech. Phys. Solids, v. 16, 1-12.
- [8] McClintock, F.A., Kaplan, S.M., and Berg, C.A. (1966), "Ductile Fracture by Hole Growth in Shear Bands," Int. J. Fracture Mech., v. 2, 614-627.
- [9] Slocum, A.H., and McClintock, F.A. (1984), "User's and Programmers' Manuals for ASYMCR, to Predict Fully Plastic Mode II Asymmetric Crack Growth," Research Memo 263, Fatigue and Plasticity Laboratory, Massachusetts Institute of Technology, Department of Mechanical Engineering, Cambridge, MA.
- [10] Rice, J.R., Drugan, W.J., and Sham, T.L. (1980), "Elastic-Plastic Analysis of Growing Cracks," Fracture Mechanics: 12th Conference, ASTM STP 700, Am. Soc. Test Mat., pp. 189-221.

Table 1 Mode II Non-Linear Singularity Coefficients $I_{1/n}(M^P = 0)$ and
 Normalized Strain $\tilde{\epsilon}_{ij}(\theta = 0, M^P = 0)$ from Shih [4] .

Strain hardening exponent n	$I_{1/n}(M^P = 0)$	$\tilde{\epsilon}_{ij}(\theta = 0, 1/n, M^P = 0)$
0	0.59	0.88
.1	0.72	0.88
.2	0.83	0.88
.3	0.92	0.88
.4	1.01	0.88

Table 2 Preliminary Experimental Data and Resulting Fracture Strain.

(Displacements to initiation, u_i , and then to final separation, u_f , from surface lengths s_1, s_2 .)

Alloy, comp. %, treatment, hardness	Crack Surface Observations			Crack Growth	Displacement Ratio	Initial Displacement	Flow Properties (estimated)	Fracture Strain
	s_1 mm	s_2 mm	ρ mm	$\frac{\Delta c}{\rho} = \frac{s_1+s_2}{2\rho}$	u_f/u_i Figs. 5, 6	$u_i = u_f/(u_f/u_i)$ $= (s_2-s_1)/(u_f/u_i)$ mm	$\frac{2(E-1)}{k_{yield}}$ expon n (estimated)	γ_c Eq. 46
1018 steel Fe, 0.2 C, cold finished, 133 Bhn	2.1	2.4	0.005- 0.020	450- 113	78.7- 27.7	0.00381- 0.01083	2.266 0.09	0.887- 0.648
6061-0 aluminum .6 Si, .25 Cu, 1. Mg, .25 Cr, annealed, 30 Bhn	2.7	3.0	0.01- 0.02	285- 143	52.8- 33.5	0.00568- 0.00896	2.60 0.16	0.581- 0.474
6061-T6 alum. quenched, aged 95 Bhn	2.0	2.0	0.005- 0.02	400- 100	70.7- 25.2	0.0 0.0	1.87 0.13	0.0 0.0

LIST OF FIGURE CAPTIONS

- Fig. 1a. Asymmetrically cracked part
- Fig. 1b. Idealized asymmetric crack specimen
- Fig. 2. Strain ahead of a growing crack
- Fig. 3. Damage site spacing for $\Delta c = \rho$
- Fig. 4. Cumulative strain distributions ahead of a growing crack for $\Delta c / \rho = 0.125$
- Fig. 5. Small scale crack growth versus displacement for various step sizes, and for the quasi-steady approximation with various strain hardening exponents
- Fig. 6. Large scale crack growth vs. displacement for $\Delta c / \rho = 0.125$, and quasi-steady approximation with $n = 0.1$

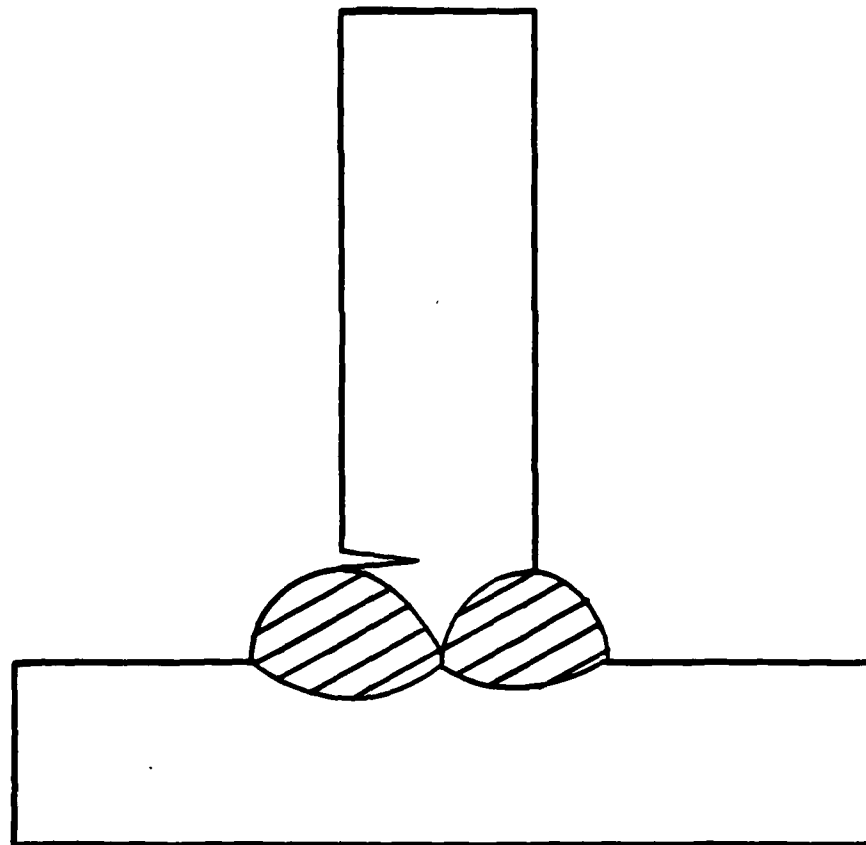


Fig.1a. Asymmetrically cracked part

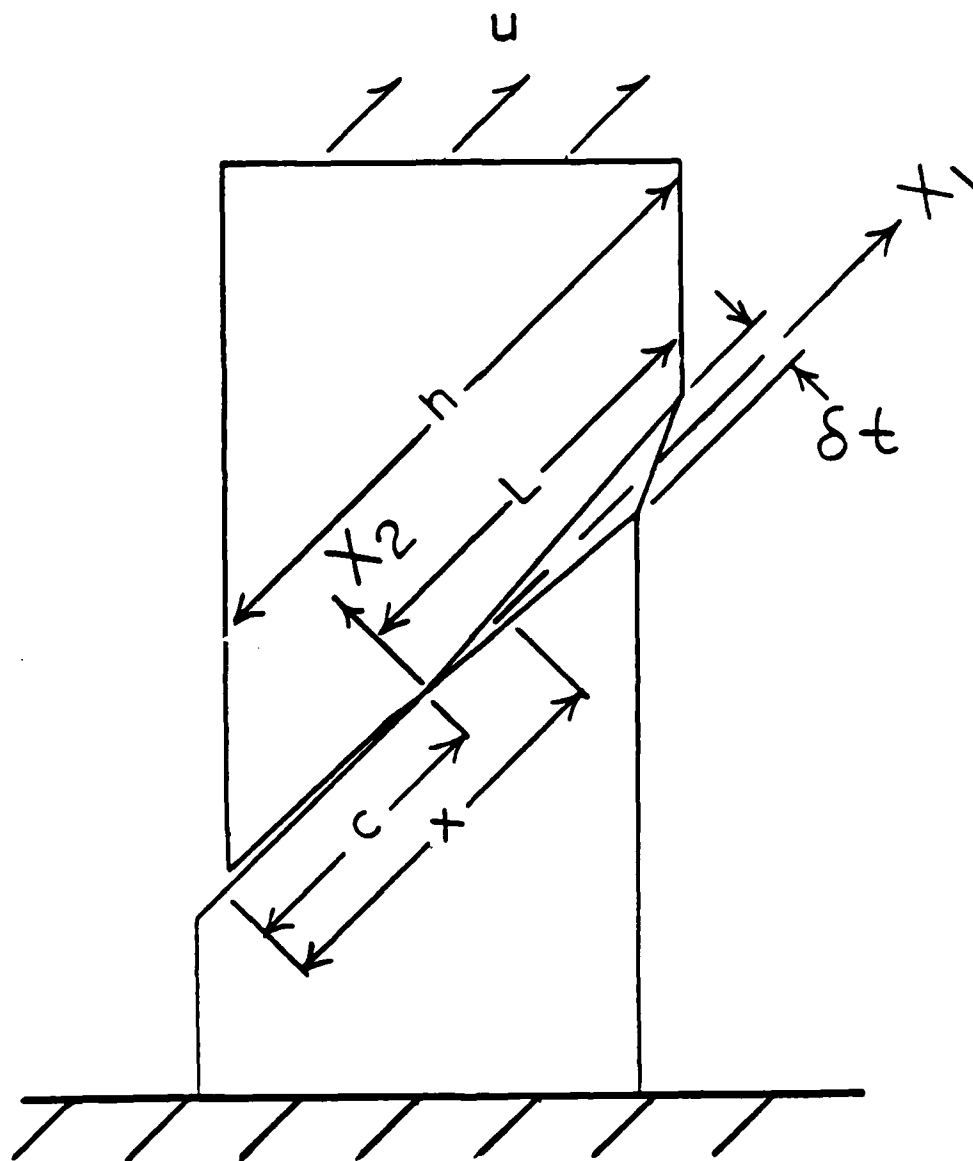


Fig.1b. Idealized asymmetric crack specimen

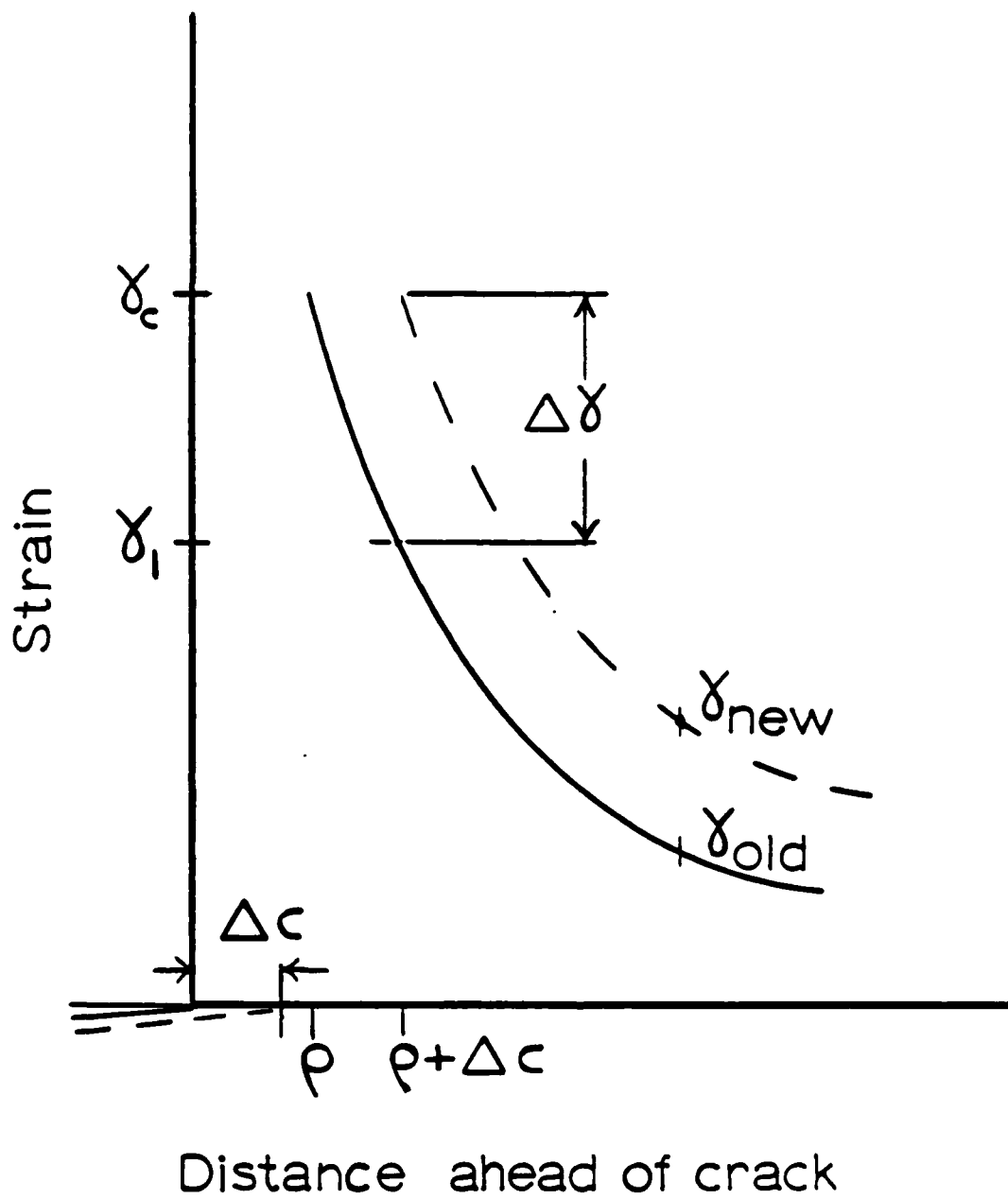


Fig.2. Strain ahead of growing crack

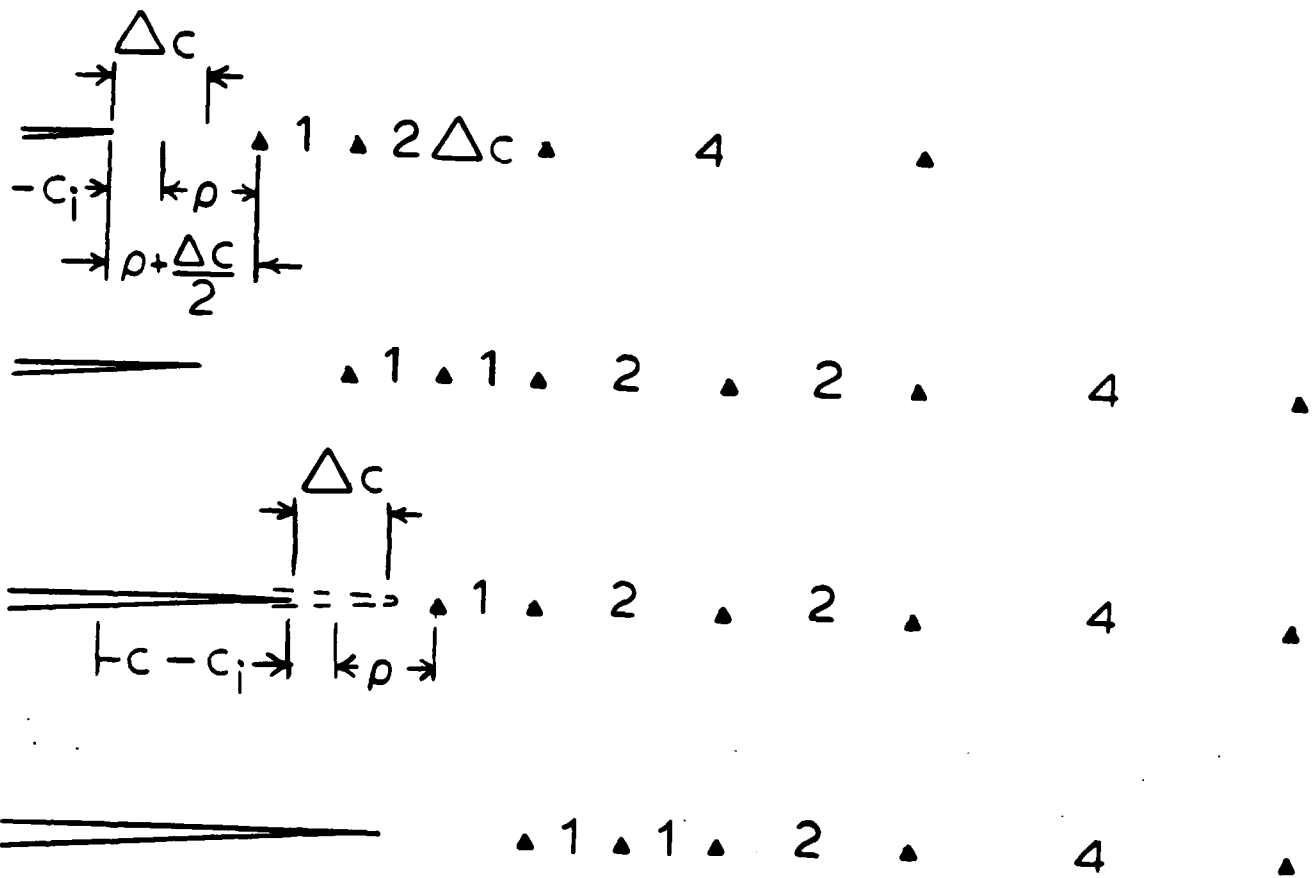
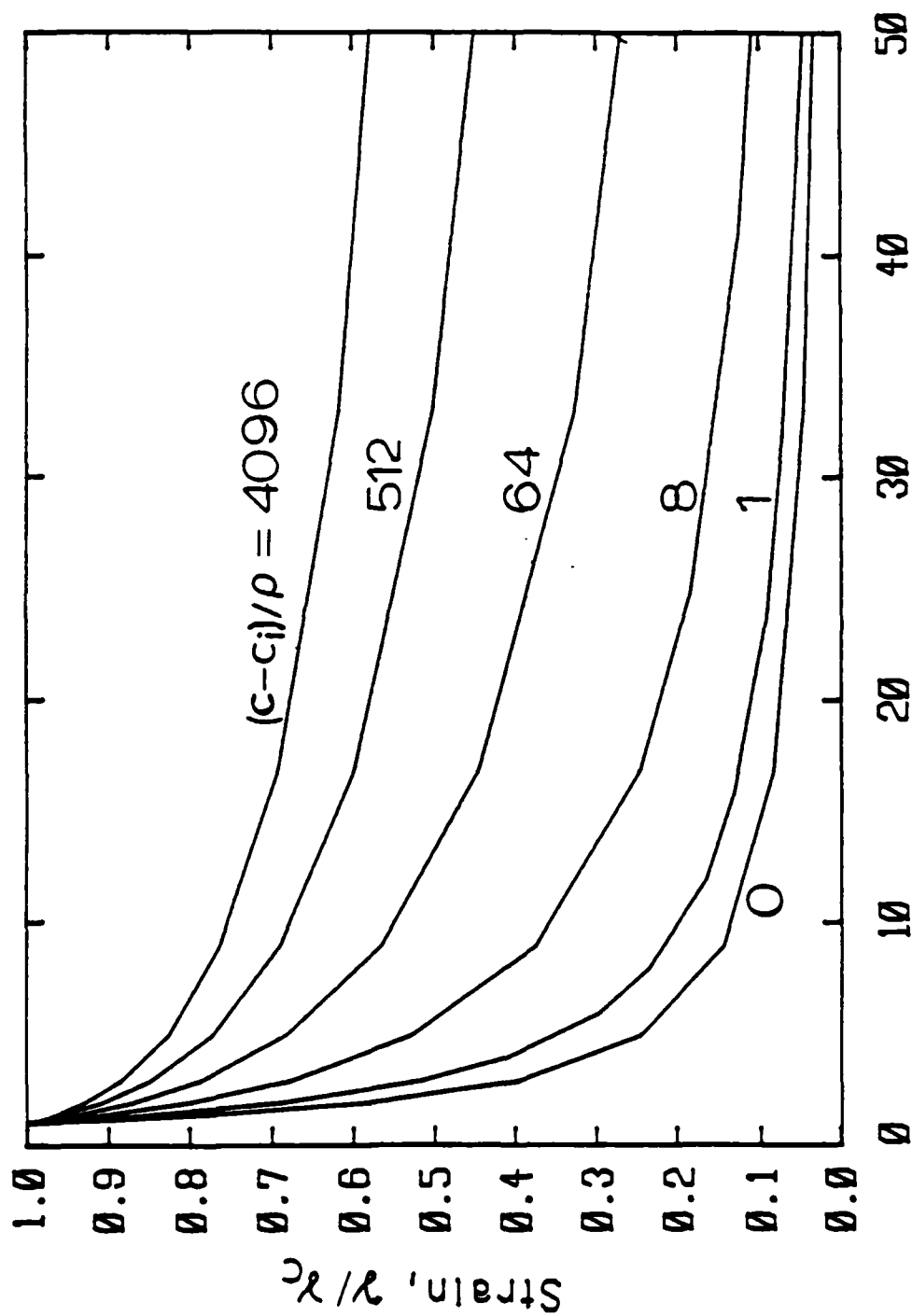
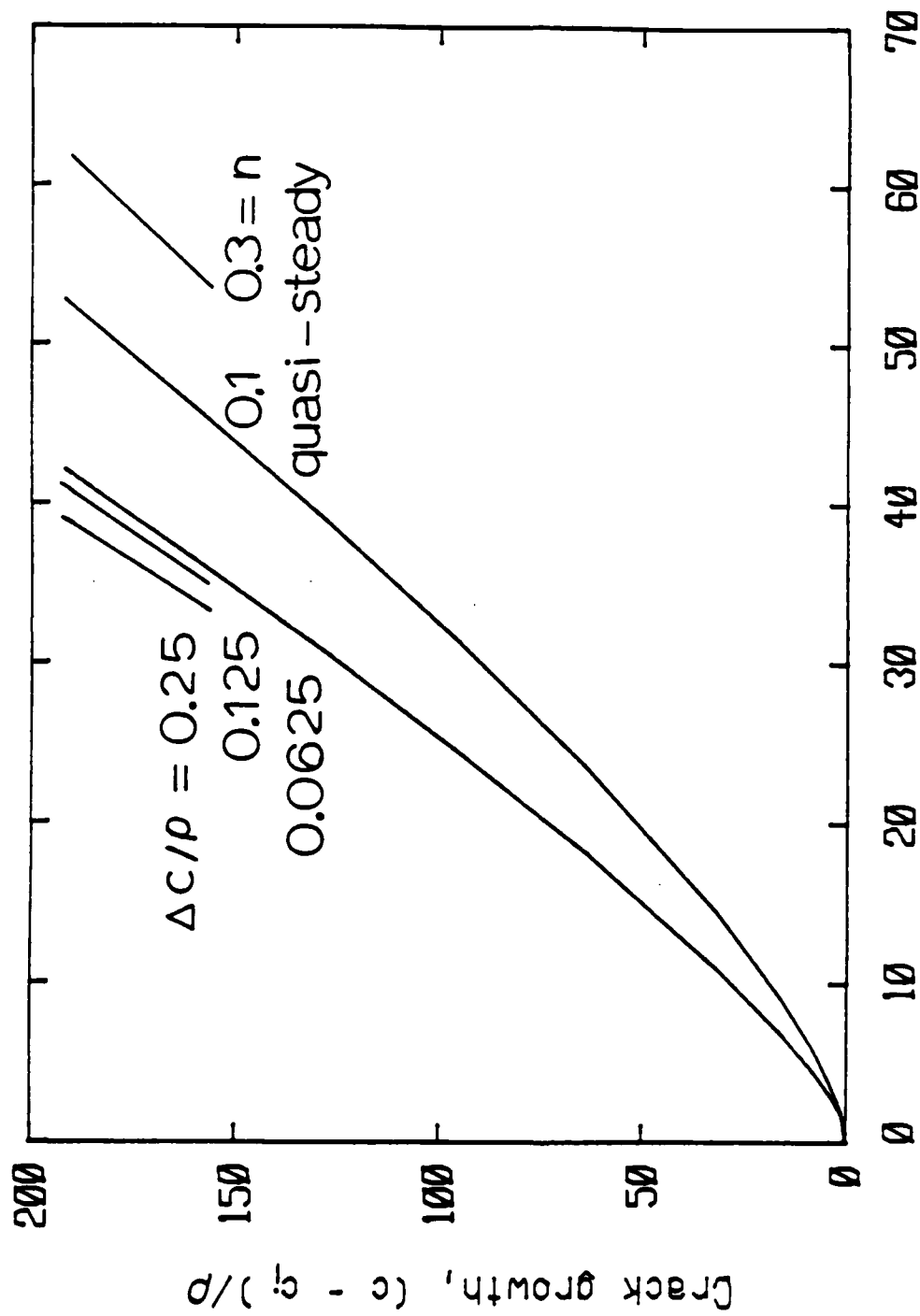


Fig. 3. Damage site spacing for $\Delta c = \rho$



Distance ahead of crack, r/ρ

Fig.4 Cumulative strain distributions ahead of a growing crack, $\Delta c/\rho = 0.125$.



Displacement, u/u_f and u_{qs}/u_f

Fig.5 Small scale crack growth versus displacement for various step sizes and for the quasi-steady approximation with various strain hardening exponents.

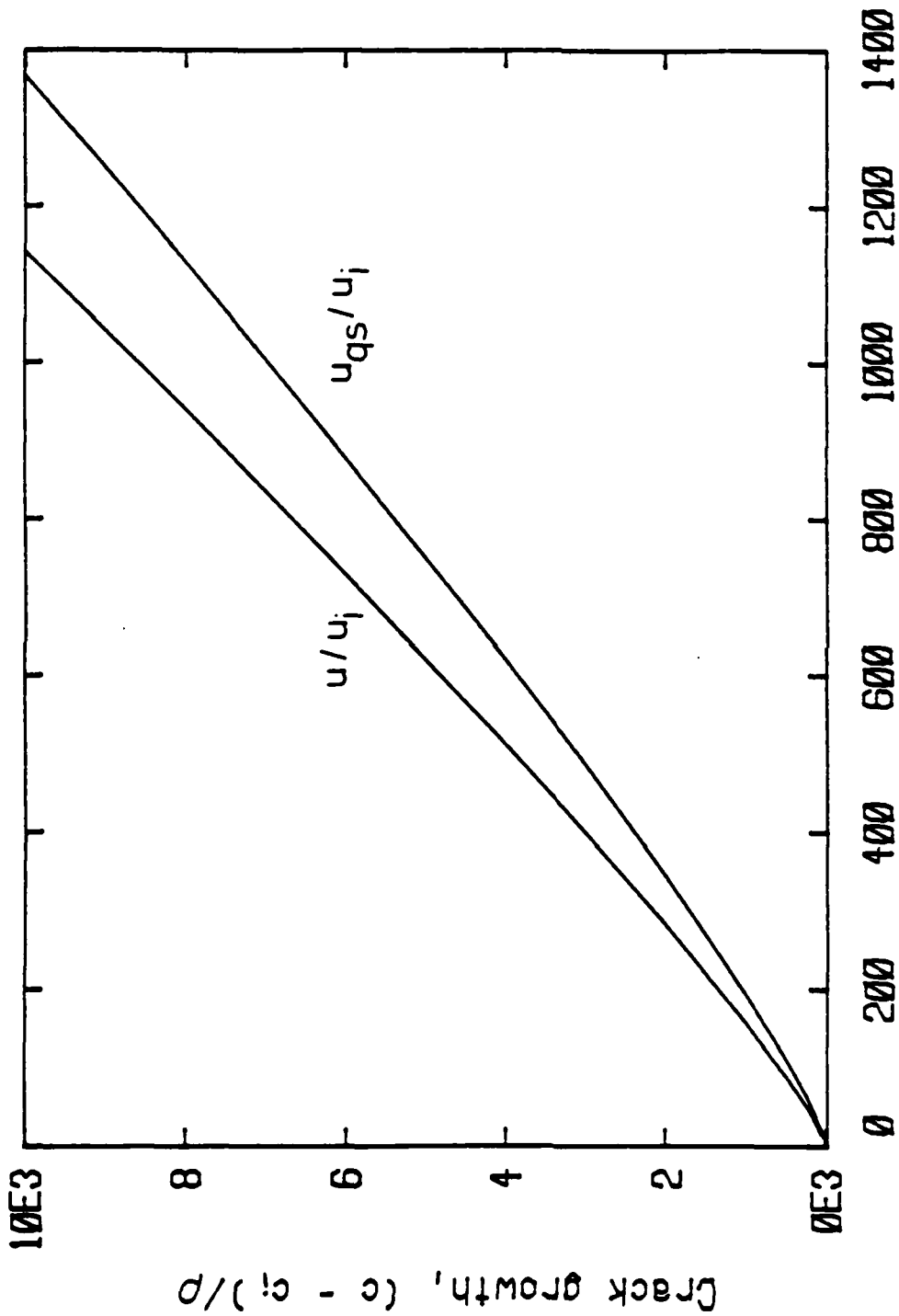


Fig. 6 Large scale crack growth vs. displacement for $\Delta c/\rho = 0.125$ and quasi-steady approximation with $n = 0.1$.

END

FILMED

4-85

DTIC

